OPTIMIZATION OF MICRO PIN-FIN HEAT SINK WITH STAGGERED ARRANGEMENT

by

Kozhikkatil Sunil ARJUN and Rakesh KUMAR***

Department of Mechanical Engineering, Indian Institute of Technology (ISM), Dhanbad, India

Original scientific paper
https://doi.org/10.2298/TSCI161221202A

The effect of the pin-fin shapes on the overall performance of the carbon nanotube bundles as porous micro pin-fins with in-line and staggered arrangement for the heat transfer and pressure drop is studied using FLUENT 15.0. The results of the study revealed that at 100 < Re < 2000, triangle has the best performance followed by square, rectangle, hexagon and circle in 1 mm height, 15 mm width, and 45 mm length silicon rectangular mini-channel. The staggered configuration gave better heat transfer performance than in-line arrangement at all Reynolds numbers for all shapes with up to 19% thermal improvement but with up to 79% pressure drop differential. On a mini-channel surface with nanotube fins, the nanofluid (0.001 to 1%) increases the thermal performance up to 40% in comparison with water. The best thermal performance enhancement of 106% was obtained by using staggered triangular fins with larger fin height of 0.75 mm, smaller fin width of 0.5 mm, and spacing double the fin width and 0.01% CuO-water nanofluid followed by 103% with 0.01% Al_2O_3-water in comparison to channels with inline circular fins and water.

Key words: *electronic cooling, CFD, pin-fin, mini channels, nanofluid, carbon nanotube*

Introduction

The heat sink industry, traditionally the supplier of cooling products, is always searching for new technologies, which enhance thermal performance with no cost penalties. For this reason, a comparison of different geometries of pin-fin heat sinks is of interest and needs to be carried out to determine applicability as a general cooling product. Operating conditions for microprocessor heat sinks have become considerably simpler than in the past. The dimensions of fully ducted heat sinks of modern servers and workstations now feature narrower fin gaps approaching 1.5 mm, tall fin heights approaching 50 mm, and long flow lengths approaching 90 mm. Among the different heat sink designs proposed in the past few decades, pin-fin heat sinks are the most promising one.

An extensive amount of work has been done on the pin-fin heat sinks and researchers have developed several effective pin-fin structures, and many of these structures has been gone through the optimization procedures [1-4]. Most of the work done in the pin-fin heat sinks was confined to the macro scale until the beginning of this decade [2-4]. However, as the manufacturing techniques used in the micro scale has developed vigorously and as the electronic industry is striving towards the miniaturization of the devices, some researchers started working on

* Corresponding author, e-mail: arjun@mece.ism.ac.in

the development and optimization of the micro scale heat sinks recently [5, 6]. The height and width of the fins are affecting the thermal resistance as well as the pressure drop in the heat sink [2]. The rectangular pin-fins outperformed the circular fins in the performance of the thermal resistance [3]. Circular and elliptical pins were showing the best thermal performance and Cu was found to be the best material for the heat sink manufacturing [7]. At high Reynolds number, heat sinks with high density of pin-fins are preferred and less denser pin-fins are preferred at low Reynolds number [6]. The pin efficiency of the pin-fin heat sinks is low at micro level and this issue can be resolved by using shorter pin-fins [5]. At very low, intermediate and high flow rates circular, ellipse, and rectangle pin-fins were the best performers [8]. The thermal resistance is the dominating factor at lower and intermediate flow rates and pumping pressure is the dominating factor at intermediate and high flow rates.

An experiment performed for circular finned micro heat sink found Ag-water nanofluid perform better then Al_2O_3-water nanofluid [9]. Diamond-water nanofluid is better than Al_2O_3-water from heat transfer point of view and circular fins give the higher heat transfer rate and square fins caused higher pressure drop compared with other fin geometries [10]. Highest top wall temperature, friction factor, and thermal resistance with rhombus and smallest hydraulic diameter of the hexagon has the highest pressure drop and heat transfer coefficient among other shapes [11]. Heat transfer rates for nanofluids as a coolant are higher than water [12]. Nanofluid enhance the heat transfer, but it cause to increase the pressure drop [13]. Square pin-fins are thermally better than circle and the change in the axial pitch between the pin-fin structures show negligible effects on both the thermal and hydraulic behavior [14]. For heat sinks with circular pins, the thermal resistance of the device decreases as the axial pitch is decreased at the cost of increased pressure drop. Triangular geometry is the best shape [15]. Staggered geometries perform better than inline and at lower pressure drop and pumping power, elliptical fins work best [16]. At higher values, round pin-fin offer highest performance.

Crosscut pin-fin, straight and parallel plate fins were compared with elliptical pin-fin heat sink [7]. Cylindrical pin-fins give the best overall fan-sink performance, when only impinging flow drawn through the fin arrays was considered [17]. Round fins including the fin height to diameter ratio (h_f/d_f) and the inter-fin pitch to diameter ratio (p_f/d_f), gave a universal pressure drop result for all operating conditions and compared the performance of different pin-fin geometries [18, 19]. The optimal geometry of an array of fins that minimizes the thermal resistance between the substrate and the flow forced through the fins [20]. Staggered arrays exhibit higher element heat transfer coefficients and friction factors than inline arrays at a given flow rate [21]. Thermal performance of the staggered fin configuration was better than the planar fin configuration, however, was realized at the expense of an additional pressure drop [22]. Heat transfer enhancement mechanisms and the geometrical effects in in-line and staggered parallel plate fin heat exchangers were examined [23]. Tip clearance, span wise spacing across a range of approach flow rates, and fin densities [24]. Effect of flow bypass on the performance of longitudinal fin heat sinks was studied [25]. Cooling performance of longitudinal heat sink was studied by numerical, experimental and nodal network techniques [26].

Microchannels have proven to be effective cooling systems and understanding how to achieve the maximum performance through modified channel devices and coolant is significant to keep electronic systems from malfunctioning. The carbon nanotube (CNT) microstructures, because of impressive material and mechanical properties built onto the surface of microchannels as pin-fins need to be further evaluated to maximize cooling with no cost penalties. The shape, material, size, pore density, spacing and layout of the pin-fins. Diameter of channel and

the choice of nanofluid with its concentration and size of nanoparticles are affecting the thermal resistance and pressure drop differently at different Reynolds number and their combined effect is vital. In this study, single-walled CNT (SWCNT) as a solid emerging out from surface and as porous media are modelled with Al_2O_3- and CuO-water nanofluids in single-phase regime with constant heat flux, no-slip and no interfacial resistance boundary conditions in a micro-channel. Fin height is kept half the length of the channel height with same number of fins in the row as well as spacing same as the fin width is used to maximize the cooling without minimal penalties, varying the aforesaid vital factors identified.

Problem description

Ten device geometries (in line and staggered circle, square, rectangle, triangle, and hexagon) were developed for this simulation. The A1 mm thick rectangular mini-channel made of silicon with a size of 45 mm × 15 mm is used. Carbon multi walled nanotubes (MWNT) with broad diameter distribution of 10-100 nm are used. For the fully covered, nanotubes with a diameter of 1 nm and 0.5 mm in height, were grown at the center of the silicon wafer at the bottom in a rectangular area of 25 m × 15 m as is done with all micro pin-fin arrangements. Figure 1 is the device geometry of the mini-channel with triangular staggered micro pin-fins. Flow regime is considered a continuum flow and solved using the Navier-Stokes equations.

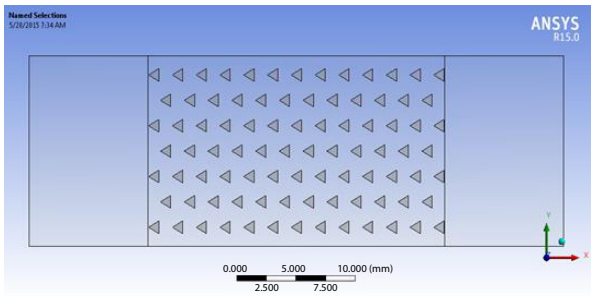

Figure 1. Mini-channel model with triangular CNT pin-fins in a staggered array

The basic governing equations for a steady-state, incompressible flow are:

– continuity equations

$$\left(\nabla \rho u\right) = 0 \tag{1}$$

– conservation of momentum

$$\rho\left(u\nabla u\right) = -\nabla p + \mu\nabla^2 u \tag{2}$$

$$\mu = \mu_0 \left(\frac{T}{T_0}\right)^{3/2} \frac{T_0 + \mathrm{S}}{T + \mathrm{S}} \tag{3}$$

– conservation of energy

$$\rho c_p \left(u\nabla T\right) = k\nabla^2 T \tag{4}$$

Simulation parameters

The 3-D meshed geometry is discretized based on the finite volume method. ANSYS FLUENT 15.0 [27] is used to model the flow past the CNT pin-fins in a staggered array in the rectangular mini-channel and solves the governing equations iteratively for each control volume. Convergence criterion for the solution is residuals of less than 10-6 for both continuity and momentum. Viscous-laminar model is enabled and the nanofluid is treated as single phase. Density, specific heat, and thermal conductivity are 1027.9 kg/m^3, 4.05 kJ/kgK, and 0.62 W/mK for Al_2O_3-water nanofluid and 1038.1 kg/m^3, 3.767kJ/kgK, and 0.637 Wm/K

for CuO-water nanofluid used in the present study. The fluid properties are kept constant throughout the simulations. Each model contained a fine mesh surrounding the finned section with a less dense mesh as the channel extends to the inlet and outlet. In order to optimize the micro pin-fins using multiple flow rates and heat fluxes: varying height of fins, fin width and spacing, and applying multiple material properties to the pin-finned geometry. A constant heat flux of 100 W/m^2 is applied to to a 15 mm × 25 m area at the bottom of the channel. The flow is ensured hydrodynamically developed before the fluid reaches the heated region. Transverse and longitudinal spacing of the fins for this study is equal to double the width of the fin and fin height is kept half the channel height or 0.5 mm. For all geometries, the fin material property used is that of SWCNT. However, because the thermal conductivity is unknown when nanotubes are clustered together to form fins, an effective thermal conductivity of 400 W/mK is used [28].

The CNT fins are modeled as a solid emerging out from surface rather than bundles of nanotubes. The CNT micro pin-fins are made up of many nanotubes where the fluid penetrates through small gaps, or nanochannels, allowing for an increased in convection within the system. As shown in [29], CNT absorb the fluid at high temperatures creating a porous like material and increases heat transfer due to a hastened nucleate boiling onset initiating phase change. This assumption in the model may underestimate the thermal performance of CNT solid fins. Also, there are ongoing investigations of the effective thermal conductivities of CNT bundles. Therefore, an estimation of an effective thermal conductivity is used. Hence, the best performance case is simulated using porous medium. This study was simulated using multiple flow rate inputs. Initial inlet temperature and outlet static pressure values applied to the model are assumed for all simulations to be 25 °C and 0 Pa, respectively. To monitor the heat transfer coefficient and the heat transfer rate, the outer walls of the channel are set to be adiabatic. No-slip boundary conditions and no interfacial resistance are assumed at the wall/fluid interface. Water is used as the working fluid flowing through this heat exchanger with different velocities through the inlet of the channel. Thermal resistance with Re 2000 at grid numbers 353638, 382366, and 456016 are found to have same value of 2.6. Numerical results and experimental data [30] were quite close (2.65 for Re 2000 with less than 2% deviation) and hence fine numbers of grid (456016) are chosen.

Using the different geometry and CNT material properties, channel clearance is varied using fin to channel height ratios between 0.25-0.75. This study is designed to understand the optimum fin height with respect to the channel and is compared to the channel with no fins. The spacing are kept equal to double the fin width. The height of the fins to the channel height is kept at half the channel clearance and the number of fins along each row varies based on the width and the spacing of the fins. Fin width is varied from 0.5-2.5 mm. Once the optimum size of fins is determined, the spacing is varied using the fin's width of 1.25 mm. Unlike the previous spacing that is the same as the fin width, the spacing is reduced to 2 mm and 2.25 mm while maintaining the same number of fins in the row. These were all compared to the smooth, unfinned channel. The same pin-fin geometry is used similar to the first study with the fin width at 1 mm, spacing at 2 mm, and the fin height half of the channel height. Silicon, copper, and aluminum are also used as the fin material.

Water flows past pin-fins carrying heat subjected by bottom surface. With constant heat flux, different geometry of nanotube bundles and forced convection, the temperature across surface of the microchip and bulk temperature of fluid vary. To accurately obtain heat transfer coefficient, h, across the microchip region for simulations, an average h was obtained. There were some uncertainties within the model that can increase the error in the

approximation. As the scales start moving toward micro or nanoregime, conventional continuum calculations can no longer be used. In addition, resistance created at interface of CNT and working fluid is still a major issue. Influence of Al_2O_3-water and CuO-water nanofluids on the thermal performance in comparison with cases of no nanotubes and with nanotube fins using water are also investigated.

Validation

To validate, experimental results taken from work completed for a heat sink containing 625 square micro pin-fins of 445 μm × 445 μm in a staggered array was solved with water used as the working fluid flowing with Reynolds number ranging from 60-800 [31]. The fins and channel have a height of 3 mm. The longitudinal and transverse spacing of the fin measured 565.7 μm. The ambient fluid temperature is initially at room temperature and heat is applied to the bottom surface. The Nusselt number and pressure drop, across the finned structure were calculated and compared to the experimental data shown in fig. 2 and are very similar to that of the value obtained in the experimental work for Nusselt number values and pressure drop except for Re 100 and 500 (for pressure drop alone) within 21%. This proves that present study can accurately predict the heat transfer through the channel with micro pin-fins on the surface. The, ϕ, is the volumetric concentration of the particles in the nanofluid which in this case is $\phi = 0.01$. Computational simulation involves mono-sized particles, whereas particles with a range of particle sizes are used in the experiments, thus leading to differences in inter particle frictional forces. Which might be the reason for such deviations in experimental and computational pressure drop values.

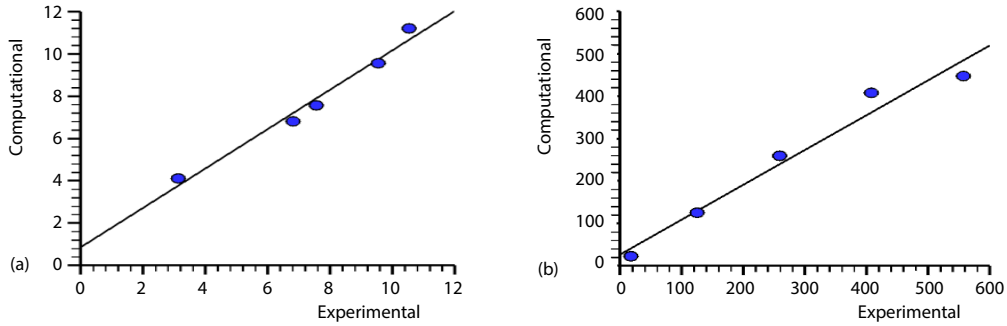

Figure 2. Validation of simulated data of staggered square pin-fins at different Reynolds number; (a) Nusselt number, (b) pressure drop

Results and discussion

Average Reynolds and Nusselt numbers are collected for the different inputted heat fluxes and flow rates. Average axial velocity was obtained as the fluid flowed across the fin bank:

$$\mathrm{Re} = \frac{\rho u D_c}{\mu} \tag{5}$$

Nusselt number is proportional to the average heat transfer coefficient, h, and the hydraulic diameter of the channel, and inversely proportional to the thermal conductivity, k:

$$\mathrm{Nu} = \frac{hD_c}{k} \tag{6}$$

Average heat transfer coefficient is obtained from the surface area of the fins and the base that the fluid interacts with. The expression:

$$h = \frac{h_{\text{fin}} A_{\text{fin}} + h_b A_b}{A_{\text{fin}} + A_b} \tag{7}$$

where h_{fin} and h_b are the heat transfer coefficients of the fin and the base of the heated region only, A_{fin} and A_b are the surface areas in which the fluid touches the fin and the heated base region, respectively. The heat transfer coefficient of the fin and the base at the fluid interface is obtained:

$$h = \frac{q}{T_w - T_{nw}} \tag{8}$$

where q is the wall heat flux, T_w – the temperature of the wall, and T_{nw} – the near wall temperature.

Pressure drop is determined across the pin-fins only to avoid any entrance and exit effects of the fluid-flow using a maximum axial velocity. Three different mesh sizes with triangular elements are applied in the grid test for solid pin-fins at Re = 100 using standard wall functions, achieved by refining the mesh. Triangular elements were selected as they were more robust and the solutions required less grid refinement to obtain stable outlet bulk temperatures. The solution is tested for 2000×60 (305.49 K) and 2000×90 (305.44 K) grid sizes and it was noted that decreasing the 2000×75 (305.45 K) does not result in any considerable difference in outlet bulk temperature and hence chosen as the optimal size. Mesh configurations of 2000×75 ensured grid independence and is used for further simulations.

Different shaped micro fins

For the same Reynolds number, the devices with the MWNT perform better than the device with no MWNT. Similar to the results by Shenoy *et al*. [29] for the finned device, the surface area is much higher than the device with no MWNT and therefore more heat is removed. The Nusselt number with respect to the rectangular mini-channel surface area of 375 mm^2 without fins was found to be 20.29 and the Nusselt number with respect to the above area with triangular fins of MWNT having a total surface area of 420.5 mm^2 was 21.51, with the use of 0.01 per cent CuO-water nanofluid. Results of different shaped finned microstructures of inline configuration on surfaces of mini-channels are compared to the staggered finned channel. With increasing Reynolds number, Nusselt number values increase for all mini-channel simulations. The Nusselt number for the triangle and square shaped fins have similar values with a maximum average Nusselt number difference of 1.4% for higher Reynolds number. For this data, triangular shaped fins showed better thermal performance. The circle shaped portrayed a thermal performance which is least effective than the triangle shaped fins by about 15% for inline and 8% for staggered at lower Reynolds number with a maximum difference of 19%. Rectangle and hexagon are more efficient than the circle with rectangle still better than hexagon. For lower Reynolds number, the Nusselt increase is high compared to that at higher Reynolds number with the gap decreases to have a 15% performance enhancement for the circular shaped fins. Figure 3 reflect the results of this study. The staggered triangular shape registered a 4% higher Nusselt number in comparison to its inline arrangement. The staggered configuration registered higher Nusselt number and pressure drop values for all fin shapes.

With the addition of fins, there is an increase of pressure drop. A value too high can create problems for the pumps to flow-fluid through the mini-channel. As the velocity increases, the pressure drop increases for all models. The triangle pin-fin curve has the highest pressure

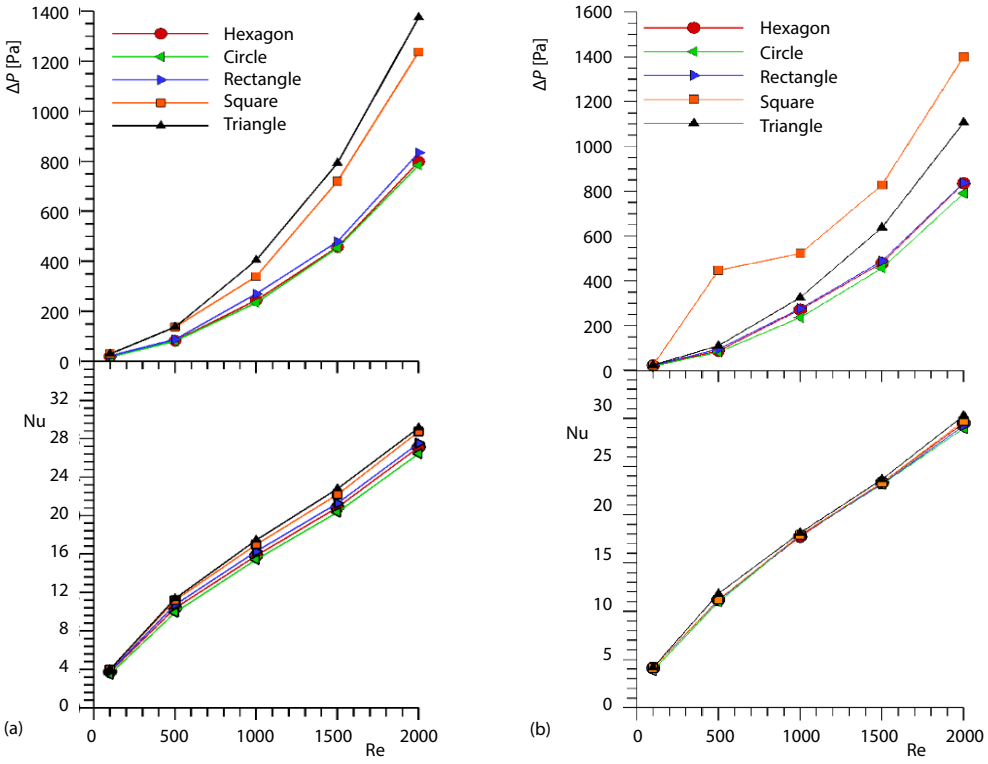

Figure 3. Fin geometry: Nusselt number and pressure drop *vs.* Reynolds number; (a) in-line, (b) staggered (*for color image see joutnal web site*)

drop with up to about 1.4 kPa followed by the next shape: square. Lowest recorded circle shape yields a maximum pressure drop of 0.8 kPa for the same Reynolds number with a 79% decrease. The aerodynamic shapes reveal a lower pressure drop because there is less separation of the fluid from the solid body. The opening between the fins disrupts the momentum and the trailing edge of the thermal boundary-layer of each oblique fin. This causes the leading edge to re-develop allowing the flow to remain in the developing state. The additions of fins show a big impact in the performance of the heat exchanger. The staggered triangular shape registered a 24% higher pressure drop in comparison to its inline arrangement.

Different micro fin height

Figure 3 display the results for different channel clearances. With increasing fin height, the thermal performance increases with increasing Reynolds number. From the lowest fin height at 0.25 mm, compared to the unfinned channel, the Nusselt number increase is high at low Reynolds number (33%) and the gap decreases to 23% for high Reynolds number. From the largest channel clearance of 0.75 mm to the smallest of 0.25 mm, there is a Nusselt number increase of 23%, fig. 4. As the fins height is increased, the pressure drop drastically increases. Pressure drop from the largest channel clearance is 3 kPa and the smallest channel clearance decreases to 0.6 kPa. Because there is a large pressure drop difference for the increasing height and the small Nusselt number relative increase, the suggested fin height is dependent on the available pump parameters used within the cooling apparatus.

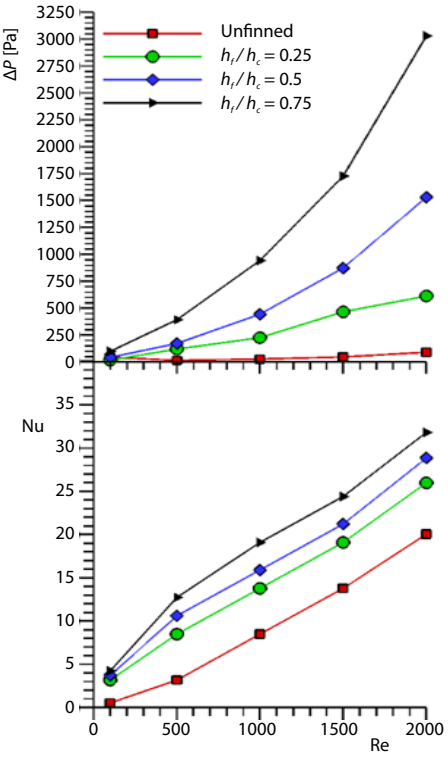

Figure 4. Ratios of fin height to channel height: Nusselt number and pressure drop *vs.* Reynolds number

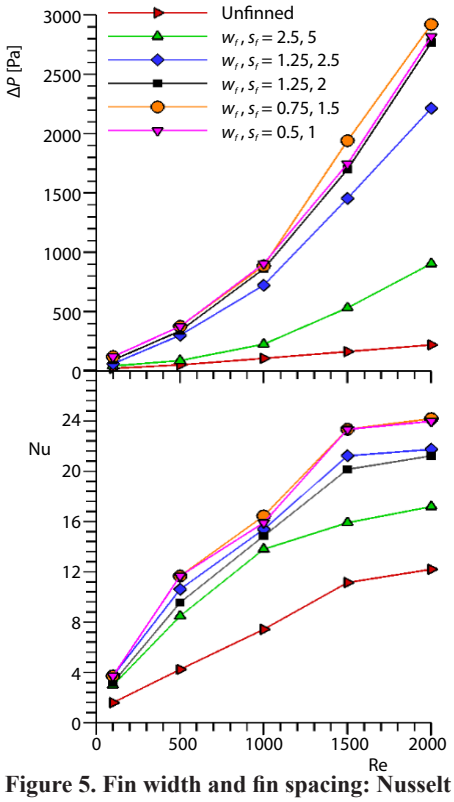

Figure 5. Fin width and fin spacing: Nusselt number and pressure drop *vs.* Reynolds number

Different micro fin width and spacing

With smaller fin width and spacing, *i. e.* number of fins was higher; the Nusselt number value was greater than other fins. Fins with width of 0.5 mm projected an 97% higher Nusselt number values than the unfinned channel and 40% higher Nusselt number values than the lowest curve of fins width and spacing at 2.5 mm. Fins with width 2.5 mm still yield a higher Nusselt number value about 41% greater than the unfinned channel with higher Reynolds number. This was shown in fig. 5.

While the smaller fin width and spacing provides higher performance, pressure drop between across the fins is sacrificed. As the fin dimensions are reduced, the pressure drop increases. Fins with width of 0.5 mm and spacing of 1 mm, the pressure drop is about 211% compared to the bigger fin width and spacing of 2.5 mm and 5 mm which has about 309% compared to the unfinned channel. The corresponding graph displaying these results is fig. 4. The bigger fins express a smaller pressure drop across the channel. This is probably due to the fewer disturbances the fluid has within the channel. It is interesting to note that for both the pressure drop and the Nusselt number the fins with width of 0.5 mm and 0.75 mm are very similar. The optimum fin width is capped out between these two widths. Similar to the other conclusion, specification of the pump parameters should be taken into account on the number of fins the system can have before the pressure drop is too high. From the results shown in fig. 4, as the spacing was closer to equal the fin width, the performance was greater. From the

smallest spacing to the largest, *i. e.* 2 mm to 2.5 mm, there was a 3% thermal enhancement for larger fins spacing. With a decrease in fin spacing, the pressure drop increases. There is about 25% increase in pressure drop from the 2.5 mm spacing to the 2 mm. From the results, it can be concluded that with decrease in width/spacing creates higher thermal performance with a sacrifice in pressure drop. By only changing the spacing, the maximum spacing yields a higher thermal performance providing a minimal pressure drop.

The parameter relating the performance of roughened channel, f, with that of smooth channel, s, representing both heat transfer (Nu), and pressure drop (friction factor, f) characteristics is made use of in presenting the results using the equation:

$$\varepsilon = \frac{\dfrac{\mathrm{Nu}_f}{\mathrm{Nu}_s}}{\left(\dfrac{f_f}{f_s}\right)^{1+3}} \tag{9}$$

The thermohydraulic performance parameter, ε, obtained in the present study is 1.45, 2.06, 1.04, and 0.9 for Re = 100, 500, 1500, and 2000, respectively. This shows that the use of fins were feasible in the present study at all Reynolds number values except at Re = 2000.

Different micro fin materials

For single-phase flows, changing material properties show little variation within the Nusselt number values, yet, they are still larger than unfinned channel. The results portraying this study are shown in fig. 6. These findings show that the chosen fin material had little effect on the Nusselt number values (5-8%). In this study, CNT are modelled as a porous media that contain small gaps where the fluid can penetrate. The nanotubes can also initiate nucleation sites initiating boiling and therefore enhancing heat transfer. Pressure drops display no difference between the fin materials because the geometry remained the same for this section of the study. Pressure drop for these studies have shown critical in optimizing fin geometry and topology. For a single phase, laminar, flow through a mini-channel, Nusselt number values for pin-fins did show improvement compared to the unfinned channel. However, various shapes, heights, widths and spacing only show significant deviation.

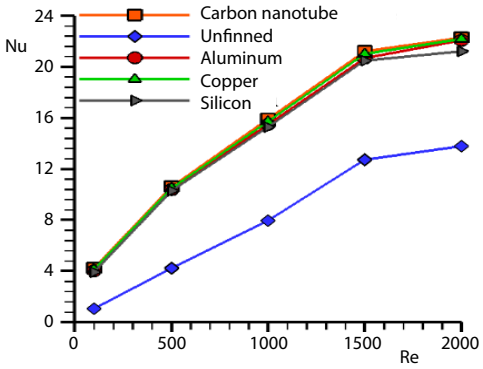

Figure 6. Nusselt number *vs.* Reynolds number for selected fin materials

Effect of use of nanofluids

The finned MWNT device has a thermal enhancement and pressure drop increase of about 103% using 0.01% volume concentration of Al_2O_3 nanofluid with respect to the same device using de-ionized water, fig. 7. The channel with finned MWNT had increases of 106% Nusselt number for the same base temperature compared to the channel with no MWNT using CuO nanofluid, fig. 7. The increase was observed in these channels having surface defects in the form of MWNT, probably due to the presence of the Brownian motion and nanoconvection in which the nanoparticles take part. The pressure drop obtained using the nanofluid for each

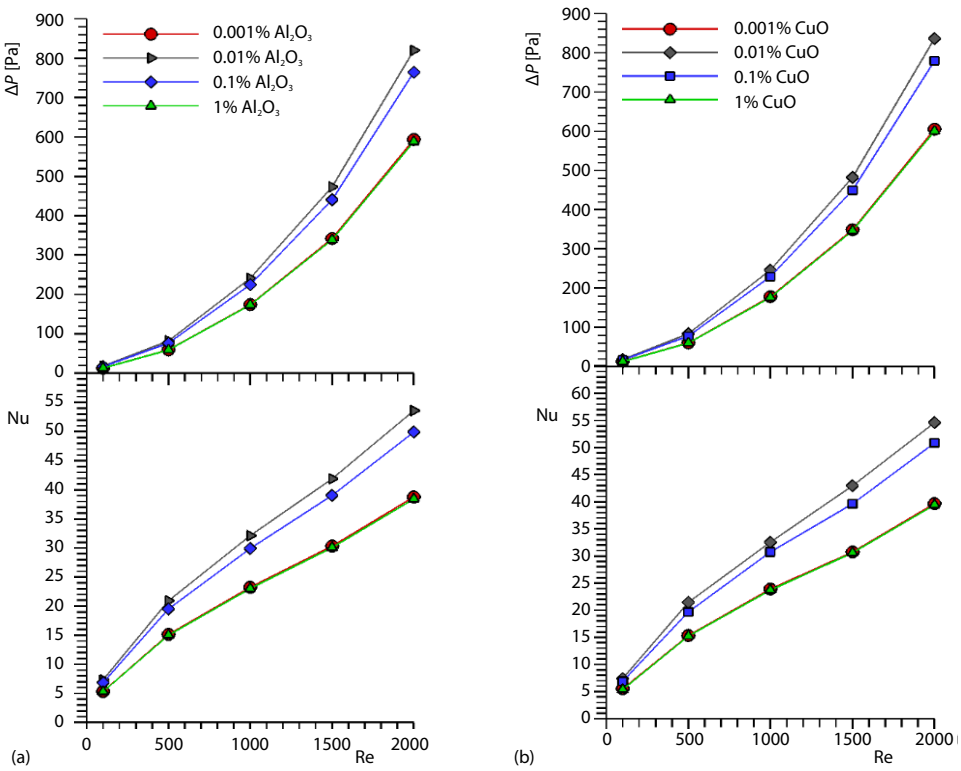

Figure 7. Effect of nanofluids on use of fins; (a) Al_2O_3-water nanofluid, (b) CuO-water nanofluid

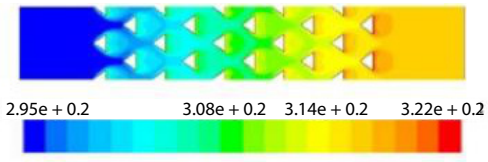

Figure 8. Temperature contour with triangular fins

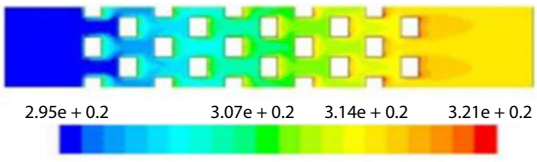

Figure 9. Temperature contour with square fins

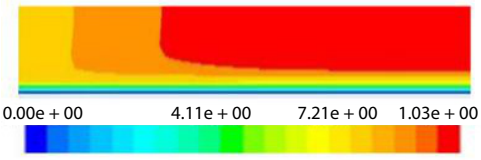

Figure 10. Temperature contour with no fins

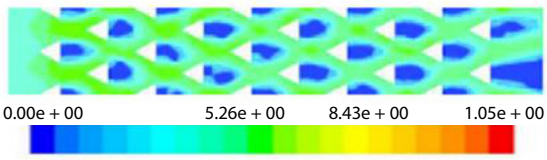

Figure 11. Velocity contour with triangular fins

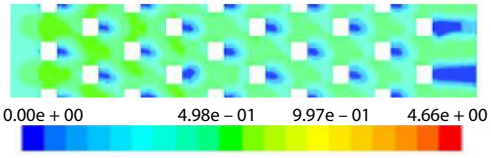

Figure 12. Velocity contour with square fins

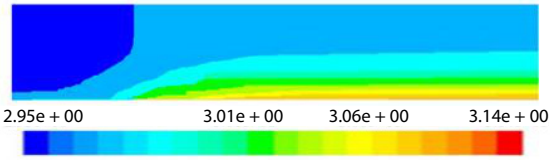

Figure 13. Velocity contour with no fins

All figures are in color (see journal web site)

channel show lower values with the addition of nanoparticles. Similar to the results for water, finned MWNT device caused higher pressure drops when compared to the no MWNT. This is due to the difference in hydraulic diameters created by the protruding MWNT on the surface. Higher pressure drops were also noticed for CuO nanofluid (40%) in comparison to Al_2O_3 (39%) nanofluid.

The hydrodynamic and thermal behaviour studied in terms of velocity and temperature contours at Re = 500 passing through the centreline in the flow direction of the rectangular mini-channel without fin and also with triangular and square shaped pin-fins using 0.01 per cent CuO-water nanofluid are shown as figs. 8-13. It is inferred that the temperature is increasing along the flow direction due to heat transfer and velocity increases at side of the wall along the flow. Also, it has seen that the shape of flow differ for every geometry and triangular finned heat sink gives the better heat mixing compared to other geometry and this finding further support the result of better heat transfer enhancement with the triangular finned heat sink.

This study verifies that the major enhancement, when using nanofluids to cool heated surfaces, is the surface defects that are deposited on the surface. The feasibility of nanofluid in this study is ascertained with better heat transfer rate enhancement compared to the settling issues with nanofluids and consequent deposition as the performance ratio being higher than one in all cases except at Re = 2000. As stated [32], these particles create imperfections on the surface causing an increased wettability. The channels that already contain engineered structures increase the surface area and wettability and the thermal performance is not significantly improved.

Conclusions

The overall performance of the five different CNT heat sinks with different shaped pin-fin structures arranged in staggered and inline order was studied in this paper for different Reynolds number varying from 100-2000 using nanofluids at different concentrations inside rectangular mini-channels. In the single-phase regime, for the porous finned device using nanofluid, 106% increase in thermal performance was obtained at higher Reynolds number. The pressure drop increased significantly to a staggered triangular finned channel. However, the addition of nanoparticles had not much significant effect. Following points are worth concluding from the present results.

- Triangular finned-heat sink gives the higher cooling rate compared to other finned heat sink for all values of Reynolds number. After triangular, square, rectangle, hexagon, and circular finned heat sinks perform better in heat transfer point of view in descending order.
- Circle finned heat sink gives minimum pressure drop at all values of Reynolds number followed by hexagon, rectangle, square, and triangle. Square and triangular finned heat sink approximately has same performance in heat transfer and pressure drop.
- In all cases, staggered geometries perform better than inline to around 4%. At lower values of pressure drop and pumping power, circular fins work best. At higher values, triangular pin-fins offer highest performance.
- The rate of heat transfer is increased by using the nanofluid but the pressure drop also increases.
- Nusselt number values of fin shapes were within 19% of each other at low Reynolds number and 15% at high Reynolds number with the triangle fins registered the highest and the circle fins lowest. However, the pressure drop values are also greatly affected in the same fashion. The lowest Nusselt number value of triangular inline fin was lower than 4% when compared to the triangular staggered.

- With increasing fin height, the Nusselt number increases. However, the pressure drop also increases drastically. From the lowest tested fin height to channel ratio to the highest, the difference in Nusselt number is 23% and the pressure drop differential at higher Reynolds number is almost 2.4 kPa.
- With decreasing fin width and spacing the Nusselt number increases. However, the increase in pressure drop is significant. For fin width at 0.5 mm, there was an increase in performance to 97% higher than that of the unfinned channel and about 40% higher Nusselt number values to the larger fin width and spacing at higher Reynolds number. Pressure drop increased significantly with a 400% increase to the unfinned channel even at lower Reynolds number.
- When the spacing is made double to the fin width, the thermal performance is better by 17% with minimal pressure drop of about 50% in comparison to spacing is kept less than double the fin width at lower Reynolds number. Fin material shows little effect of 5% on fin performance.
- It was observed that on a mini-channel surface with nanotube fins. The nanofluids increases the thermal performance in channels with nanotube fins with the best (106%) by 0.01% CuO-water nanofluid followed by 0.01% Al_2O_3-water (103%) with respect to inline circular finned channels using water. The corresponding pressure drop increased with a 40% and 39% increase with Al_2O_3-water and CuO-water nanofluid, respectively.

Nomenclature

A_b – area of base, [m^2]
A_{fin} – cross-sectional area of fin, [m^2]
c_p – specific capacity, [Jkg^{-1}K^{-1}]
D_c – hydraulic diameter of channel, [m]
d_f – diameter of fin, [m]
h – heat transfer coefficient, [Wm^{-2}K^{-1}]
h_c – height of channel, [m]
h_f – height of fins, [m]
k – conductivity, [Jkm^{-1}]
p_f – inter-fin pitch, [m]
S – Sutherland constant, [K]
S_f – spacing of fins, [m]
T – static temperature, [K]
T_0 – reference temperature, [K]
T_{nw} – near wall temperature, [K]
T_w – wall temperature, [K]
u – fluid velocity, [ms^{-1}]
W_f – width of fins, [m]

Greek symbols

ρ – fluid density, [kgm^{-3}]
μ – viscosity, [kgm^{-1}s^{-1}]
μ_0 – reference viscosity, [kgm^{-1}s^{-1}]

Acronyms

CNT – carbon nanotube
MWNT – multi walled nanotubes
SWCNT – single-walled carbon nanotubes

References

[1] Chen, H. T., *et al*., Design Optimization for Pin-Fin Heat Sinks, *Journal Electron. Packag., 127* (2005), 4, pp. 397-406
[2] Park, K., *et al*., Numerical Shape Optimization for High Performance of a Heat Sink with Pin-Fins, *Numer. Heat Transfer*, *Part A*, *46* (2004), 9, pp. 909-927
[3] Park, K., *et al*., Optimal Solutions of Pin-Fin Type Heat Sinks for Different Fin Shapes, *Journal Enhanc. Heat Transf., 14* (2007), 2, pp. 93-104
[4] Abdel-Rehim, Z. S., Optimization and Thermal Performance Assessment of Pin-Fin Heat Sinks, *Energ. Source Part A*, *31* (2009), 1, pp. 51-65
[5] Kosar, A., Peles, Y., TCPT-2006-096.R2: Micro Scale Pin-Fin Heat Sinks – Parametric Performance Evaluation Study, *IEEE Trans. Compon. Packag. Technol., 30* (2007), 4, pp. 855-865
[6] Peles, Y., *et al*., Forced Convective Heat Transfer Across a Pin-Fin Micro Heat Sink, *Int. J. Heat Mass Transfer, 48* (2005), 17, pp. 3615-3627
[7] Chapman, C. L., *et al*., Thermal Performance of an Elliptical Pin-Fin Heat Sink, *Proceedings*, 10th IEEE Semi-Therm., San Jose, Cal., USA, 1994, pp. 24-31
[8] John, T. J., *et al*., Characteristic Study on the Optimization of Pin-Fin Micro Heat Sink, *Proceedings*, ASME Int. Mech. Eng. Cong. and Expos., Lake Buena Vista, Fla., USA, 2009, Vol, 9, pp. 1373-1380

[9] Dwivedi, K., *et al*., FVM Analysis for Thermal and Hydraulic Behaviour of Circular Finned MPFHS by Using Ag-H_2O Nanofluid, *Int. J. Eng. Res. Appl.*, *4* (2014), 7, pp. 64-68
[10] Hasan, M. I., Investigation of Flow and Heat Transfer Characteristics in Micro Pin-Fin Heat Sink with Nanofluid, *Appl. Therm. Eng., 63* (2014), 2, pp. 598-607
[11] Alfaryjat, A. A., *et al*., Influence of geometrical parameters of hexagonal, circular, and rhombus microchannel heat sinks on the thermo hydraulic characteristics, *Int. Commun. Heat Mass, 52* (2014), Mar., pp. 121-131
[12] Naphon, P., Farkade, L. N., Heat Transfer of Nanofluids in the Mini-Rectangular Fin Heat Sinks, *Int. Commun. Heat Mass, 40* (2013), Jan., pp. 25-31
[13] Seyf, H. R., Feizbakhshi, M., Computational Analysis of Nanofluid Effects on Convective Heat Transfer Enhancement of Micro-Pin-Fin Heat Sinks, *Int. J. Therm. Sci., 58* (2012), Aug., pp. 168-179
[14] John, T. J., *et al.*, Parametric Study on the Combined Thermal and Hydraulic Performance of Single Phase Micro Pin-Fin Heat Sinks – Part I: Square and Circle Geometries, *Int. J. Therm. Sci., 49* (2010), 11, pp. 2177-2190
[15] Ricci, R., Montelpare, S., An Experimental IR Thermo Graphic Method for the Evaluation of the Heat Transfer Coefficient of Liquid-Cooled Short Pin-Fins Arranged in line, *Exp. Therm. Fluid Sci., 30* (2006), 4, pp. 381-391
[16] Soodphakdee, D., *et al*., A Comparison of Fin Geometries for Heat Sinks in Laminar Forced Convection – Part 1: Round, Elliptical and Plate Fins in Staggered and In-Line Configuration, *Int. J. Microcircuits Electron. Packag., 24* (2001), Jan., pp. 68-76
[17] Wirtz, R. A., *et al*., Thermal Performance of Pin-Fin Fan-Sink Assemblies, *J. Electron. Packag., 119* (1997), 1, pp. 26-31
[18] Sparrow, E. M., Larson, E. D., Heat Transfer from Pin-Fins Situated in an Oncoming Longitudinal Flow which Turns to Crossflow, *Int. J. Heat Mass Transfer, 25* (1982), 5, pp. 603-614
[19] Larson, E. D., Sparrow, E. M., Performance Comparisons among Geometrically Diffrent Pin-Fin Arrays Situated in an Oncoming Longitudinal Flow, *Int. J. Heat Mass Transfer, 25* (1982), 5, pp. 723-725
[20] Bejan, A., Morega, A. M., Optimal Arrays of Pin-fins and Plate Fins in Laminar Forced Convection, *Journal Heat Transf., 115* (1993), 1, pp. 75-81
[21] Wirtz, R. A., Colban, D. M., Comparison of the Cooling Performance of Staggered and In-Line Arrays of Electronic Packages, *J. Electron. Packag., 118* (1996), 1, pp. 27-30
[22] Sathyamurthy, P., *et al*., Numerical and Experimental Evaluation of Planar and Staggered Heat Sinks, *Proceedings*, 5th Itherm., Orlando, Fla., USA, 1996, pp. 132-139
[23] Zhang, L. W., *et al*., Heat Transfer Enhancement Mechanisms in In-line and Staggered Parallel-Plate Fin Heat Exchanger, *Int. J. Heat Mass Transfer*, *40* (1997), 10, pp. 2307-2325
[24] Barrett, A. V., Obinelo, I. F., Characterization of Longitudinal Fin Heat Sink Thermal Performance and Flow Bypass Effects through CFD Methods, *Proceedings*, 13th IEEE Semi-Therm., Austin, Tex., USA, 1997, pp. 158-164
[25] Wirtz, R. A., *et al*., Effect of Flow Bypass on the Performance of Longitudinal Fin Heatsinks, *Journal Electron. Packag*., *116* (1994), 3, pp. 206-211
[26] Iwasaki, H., *et al.*, Cooling Performance of Plate Fins for Multichip Modules, *IEEE Transactions on Components Packaging and Manufacturing*, *18* (1995), 3, pp. 592-595
[27] ***, Ansys, ANSYS Fluent 15.0 Theory Guide, ANSYS Inc., Canonsburg, Penn., USA, 2013, pp. 1-780
[28] Zhong, X., *et al*., A Study of CFD Simulation for On-Chip Cooling with 2-D CNT Micro-Fin Array, *Proceedings*, Int. Symp. High Dens. Packag. and Microsys. Integ., Shanghai, China, 2007, Vol. 7, pp. 442-447
[29] Shenoy, S., *et al*., Mini-Channels with Carbon Nanotube Structured Surfaces for Cooling Applications, *Int. J. Heat Mass Transfer, 54* (2011), 25-26, pp. 5379-5385
[30] Jonsson, H., Moshfegf, B., Modeling of the Thermal and Hydraulic Performance of Plate Fin, Strip Fin, and Pin Fin Heat Sinks – Influence of Flow by-pass, *IEEE Trans. Compon. Packag. Technol*., *24* (2001), 2, pp. 142-149
[31] Liu, M., *et al*., Experimental Study on Liquid Flow and Heat Transfer in Micro Square Pin-fin Heat Sink, *Int. J. Heat Mass Transfer*, *54* (2011), 25-26, pp. 5602-5611
[32] Ahn, H. S., Kim, M. H., A Review on Critical Heat Flux Enhancement with Nanofluids and Surface Modification, *Journal Heat Transfer, 134* (2012), 2, pp. 1-13

Paper submitted: December 21, 2016
Paper revised: September 20, 2017
Paper accepted: September 22, 2017